Scientific Research and Essays Vol. 6(24), pp. 5213-5223, 23 October, 2011
Available online at http://www.academicjournals.org/SRE
DOI: 10.5897/SRE11.1366
ISSN 1992-2248 ©2011 Academic Journals

Full Length Research Paper

A study of the terrain-correction technique for the inhomogeneous case of resistivity surveys

Sedat Yilmaz[1] and Nart Coşkun[2]*

[1]Department of Geophysics, Süleyman Demirel University, 32260, Isparta, Turkey.
[2]Department of Geophysics, Nevsehir University, 50300, Nevsehir, Turkey.

Accepted 12 September, 2011

One of the main problems in resistivity surveys is the terrain effect because of which the true interpretation of the subsurface structure may be biased. There are two approaches to deal with this problem: i) terrain-correction that uses correction factors in a homogeneous earth or ii) inversion that incorporates topography. Some terrain models such as hills and slopes are used to evaluate the effect of the terrain on the 2D modelling and inversion where the finite elements method is used for the forward modelling. The least-squares inversion technique is used to estimate the resistivities within each block of the model structure. The forward modelling results indicate that the terrain topography significantly contaminates the subsurface response. The terrain-correction used to eliminate the topography effect helps to isolate the response of the real subsurface. The inversion incorporating topography also gives reliable results if correct host rock resistivity is used in the process.

Key words: Electrical resistivity, topography, modelling.

INTRODUCTION

The two dimensional (2D) structural interpretations using electric surveys made over areas with significant elevation changes can be erroneous because the observed apparent resistivity data can be biased by topography which has been theoretically studied by many authors over the last 25 years. Fox et al. (1980) used the finite elements method to estimate the terrain effect on the resistivity data where they introduced a terrain-correction procedure to reduce the effect of topography. Holcombe and Jiracek (1984) presented a 3D terrain modelling algorithm also using the finite elements method. They suggested that the corrected data could be interpreted as the response of a flat earth model. Xu et al. (1988) used a boundary element method to model the resistivity in case of a 3D terrain. Queralt et al. (1991) defined a 2D modelling approach that uses the finite elements method for a Schlumberger array parallel to the strike. Tsourlos et al. (1999) used the finite elements algorithm to investigate the effect of terrain topography on different electrode arrays. Xu et al. (2002) calculated the longitudinal electrical potential using the boundary element method over a 2D terrain in which they showed that the along-strike apparent resistivity has lesser sensitivity to the terrain variations than the sensitivity of the across-strike apparent resistivity. Using the finite elements method, Hennig et al. (2005) demonstrated the effect of dike geometry on different electrode arrays. Rücker et al. (2006) gave an efficient numerical computation of the electric potential with finite element methods in 3D and arbitrary topography. In a follow up paper, Günther et al. (2006) presented an inversion strategy for the reconstruction of conductivity from 'dc' measurements for arbitrary topography. Unstructured tetrahedral meshes are used in order to describe the topography of the measurement. Both terrain topography and subsurface structure affect the resistivity data and the relationship between these two is quite complex. There are reports showing that the effect of terrain topography may not be completely separated from that of subsurface structure using only a terrain-correction technique when especially the subsurface is complex (Tong and Yang, 1990).

And also the actual response of the subsurface structure may be disturbed by the additional processes of

*Corresponding author. E-mail: n_coskun@yahoo.com.tr.

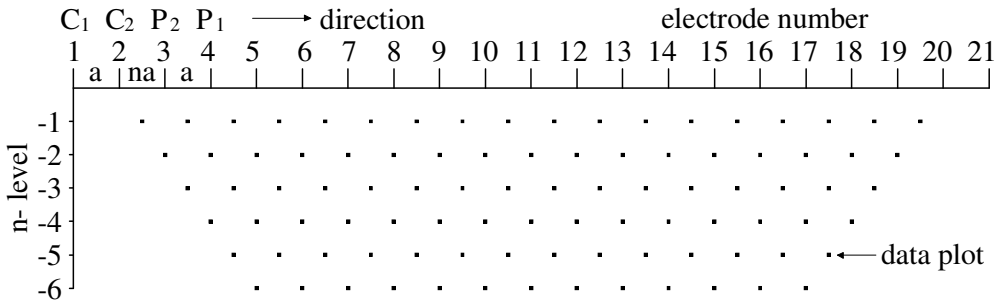

Figure 1. Dipole-dipole array and pseudo-section data plotting used in 2D resistivity surveys.

the field resistivity data. Tong and Yang (1990) presented a 2D resistivity inversion algorithm in which they use the finite elements method for the forward modelling and also incorporate the topography into the inversion process. Loke (2000) presented three different schemes to implement the inversion incorporating topography and these differ in the way that the subsurface nodes are shifted to locate the terrain topography. As shown in the literature (Tong and Yang, 1990; Loke, 2000), the terrain-correction and the inversion incorporating topography are the two methods generally used to remove the effect of the topography from the resistivity measurements. The aim of this paper evaluates the performance of two methods using the resistivity pseudosections performed with dipole-dipole electrode array (Figure 1). We describe some field procedures and also display the proposed resistivity pseudosections in homogeneous and heterogeneous media. Test inversions for the observed 2D resistivity data over topographic models are performed where the topography is incorporated into the inversion model.

INVERSION PROCEDURE

2D forward and inverse algorithms (Wannamaker, 1992) are used to model the apparent resistivity pseudosections that include topography effect. The forward modelling is based on the finite elements method which has been extensively described in many articles (Coggon, 1971; Rijo, 1977). It is easy and efficient to describe the subsurface structure and terrain topography using the finite elements mesh. The subsurface and the free-air are described by a mesh of triangular finite elements. The unknown electrical potential at element corners and the electrical properties of the element are approximated by simple linear functions. In order to solve a 2D problem, the variation in the strike direction is sorted out using a Fourier transform. It is obtained as an error substituting the linear functions into the transformed Helmholtz equation. The error between the real and approximated potential which is orthogonal to the basis functions within each element is minimized by the application of the Galerkin method. The individual element equations are assembled into a global system using these triangular elements with common nodes as follows:

$$\mathbf{Lf} = \mathbf{s} \quad (1)$$

Where the matrix $\mathbf{L}$ is calculated with the finite element mesh and resistivity model, $\mathbf{f}$ is the vector whose components are the potential values at the nodes of the mesh and $\mathbf{s}$ is the source vector whose components are zero except for the one coinciding with the source position. This system is solved using a general inverse and then the inverse Fourier transform is applied to arrive at the final potential field. The inverse equations are solved by a standard matrix solver (LLT decomposition method) or an iterative algorithm (preconditioned conjugate method). The apparent resistivity is calculated by multiplication of the potential difference with the electrode configuration factor. The inversion routine based on the damped least-squares inversion (Petrick et al., 1977) is given by:

$$\Delta\mathbf{P} = \left(\mathbf{A}^{\mathrm{T}}\mathbf{W}^{\mathrm{T}}\mathbf{W}\mathbf{A} + \lambda\mathbf{I}\right)^{-1}\left(\mathbf{A}^{\mathrm{T}}\mathbf{W}^{\mathrm{T}}\mathbf{W}\Delta\mathbf{G}\right) \quad (2)$$

Where $\Delta\mathbf{P}$ represents the vector of parameter changes, $\Delta\mathbf{G}$ is the misfit vector between the observation and calculated model response, $\mathbf{A}$ contains the derivatives with respect to model parameters, $\mathbf{W}$ is the weight matrix, λ is the damping factor and $\mathbf{I}$ is the identity matrix.

The inversion algorithm iteratively minimizes the difference between the calculated and observed apparent resistivity values while adjusting the 2D resistivity model. The subsurface is considered as a set of individual constant size blocks that have intrinsic resistivity parameters subject to the independent adjustment (Loke and Barker, 1995; Tsourlos et al., 1998).

Normalization procedure for the topographic effects

The intensity of the topographic effect depends on the unevenness of the terrain and the electrode configuration used (Tsourlos et al., 1999; Hennig et al., 2005). A technique proposed by Fox et al. (1980) can be used for correcting the apparent resistivity for topographic effects. The ratio of calculated apparent resistivity to model background resistivity can then be used to normalize the observed values in topographic correction. The normalization procedure is given by:

$$\mathrm{Ptn}_i = \frac{\rho_0}{\rho_i}\mathrm{Pt}_i,\ i = 1,2,3,\ldots,n \quad (3)$$

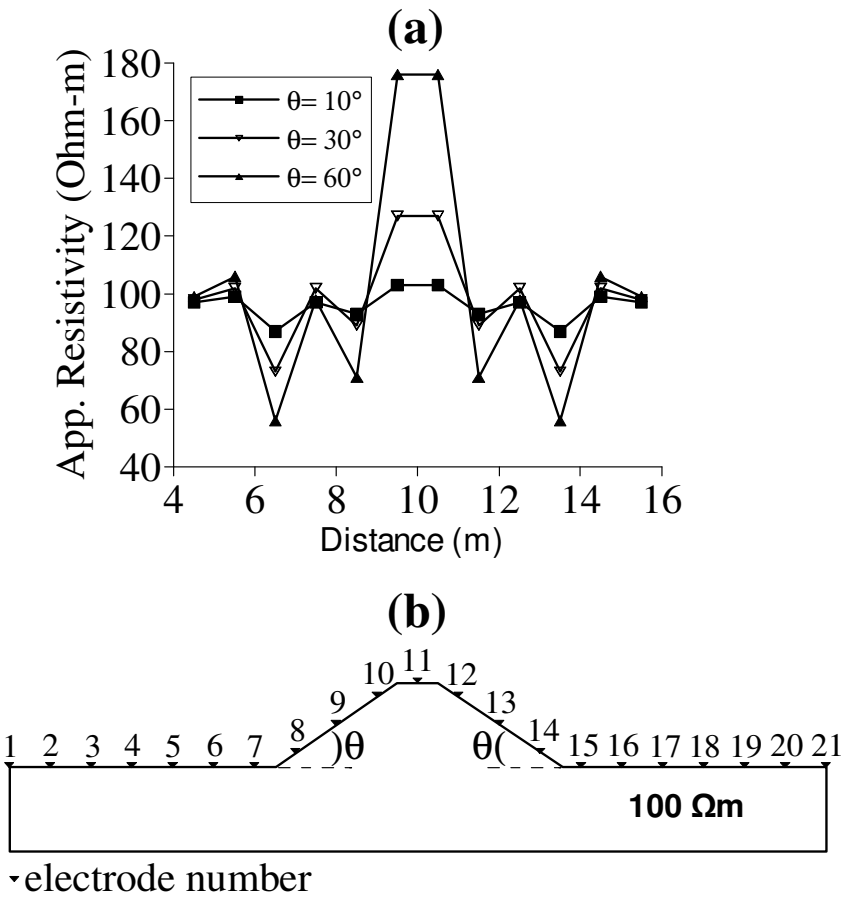

Figure 2. Topographic effect of the different hill models for dipole-dipole array. a) Apparent resistivity curves of the hill with slope angel of θ = 10, 30 and 60°. b) Hill model.

Where ρ_0 is the uniform background resistivity, ρ_i represents synthetic apparent resistivity of a homogeneous model having topography effect, Pt_i represents each observed apparent resistivity datum and Ptn_i is the corrected apparent resistivity datum.

Extensive tests performed by Fox et al. (1980) and Tsourlos et al. (1999) for simple resistivity structures with irregular topography have shown that the terrain-correction method supplies convincing results.

Modelling of topographic features

The effect of a simple topographic feature on the apparent resistivity responses along the profile shown in Figure 2a has been studied for a dipole-dipole profiling method. The topography under consideration is a hill below which the subsurface is homogeneous (100 Ωm) and the angle θ is used to characterize it (Figure 2b). Different curves in Figure 2a due to varying slope angles show the topographic anomalies where depending on the particular terrain type; the resistivity anomalies are artificially high. The apparent resistivities vary from 87 to 100 Ωm for $\theta = 10^o$, from 73 to 127 Ωm for $\theta = 30^o$ and from 56 to 176 Ωm for $\theta = 60^o$. These results indicate that the obtained resistivity data fluctuate widely when the slope value is increased. The deviations from the homogeneous half-space (that is 100 Ωm) denote the percent errors within the resistivity data with topography, that is 3 to 13% for $\theta = 10^o$, 27 to 38% for $\theta = 30^o$ and 36 to 115% for $\theta = 60^o$. Thus, the more rugged terrain the larger topographic effect. If $\theta > 10^o$, then the topography effect is significant. An example for removing the topographic effect from a resistivity pseudo-section with topography is illustrated in Figure 3. The topography model under consideration is a slope of 30° with conductive body (5 Ωm) in homogeneous subsurface (100 Ωm) (Figure 3a). The conductive body is buried at 1 m depth from the surface, having 1 m width and 1 m depth extent. The apparent resistivity pseudo-section of

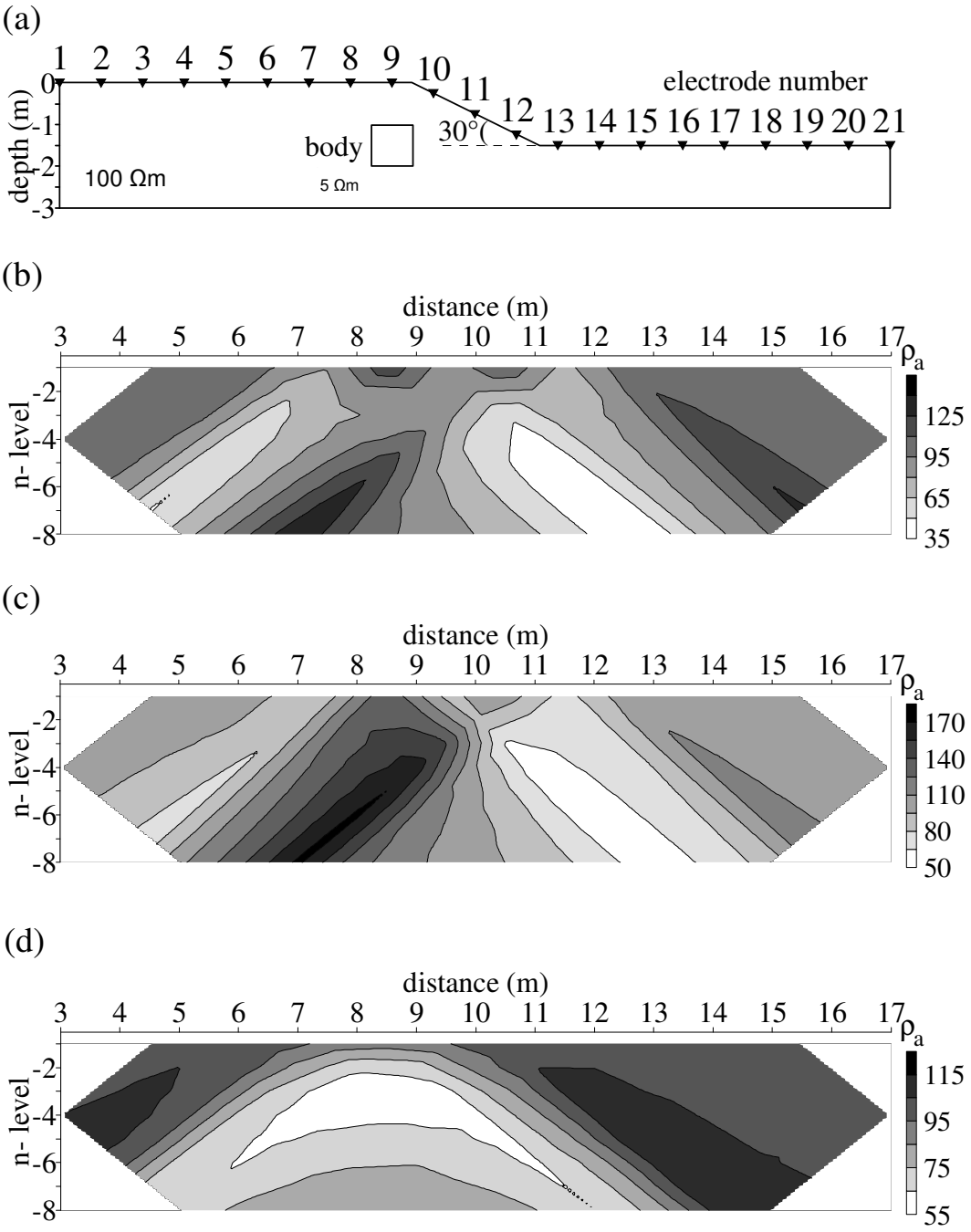

Figure 3. Pseudosections of dipole-dipole array of topography model. (a) Slope model. (b) Pseudo-section of slope model. (c) Pseudo-section of slope model without conductive body and (d) Normalized pseudo-section after application of topographic correction.

this topographic model with an anomalous body is shown in Figure 3b. The calculated data is affected not only by the buried conductive body but also by the slope surface. The terrain topography and the conductivity of the body have similar effects on the apparent resistivity (that is, the slope and the conductive body tend to produce a low resistivity). The apparent resistivities vary from 40 to 138 Ωm. The apparent resistivity pseudo-section values on the left and right are low compared to these on the centre. The apparent resistivity pseudo-section of the homogeneous topographic model without the anomalous body is shown in Figure 3c. The observed apparent resistivities for the slope model without the body have the same anomaly shape as the slope model with the body,

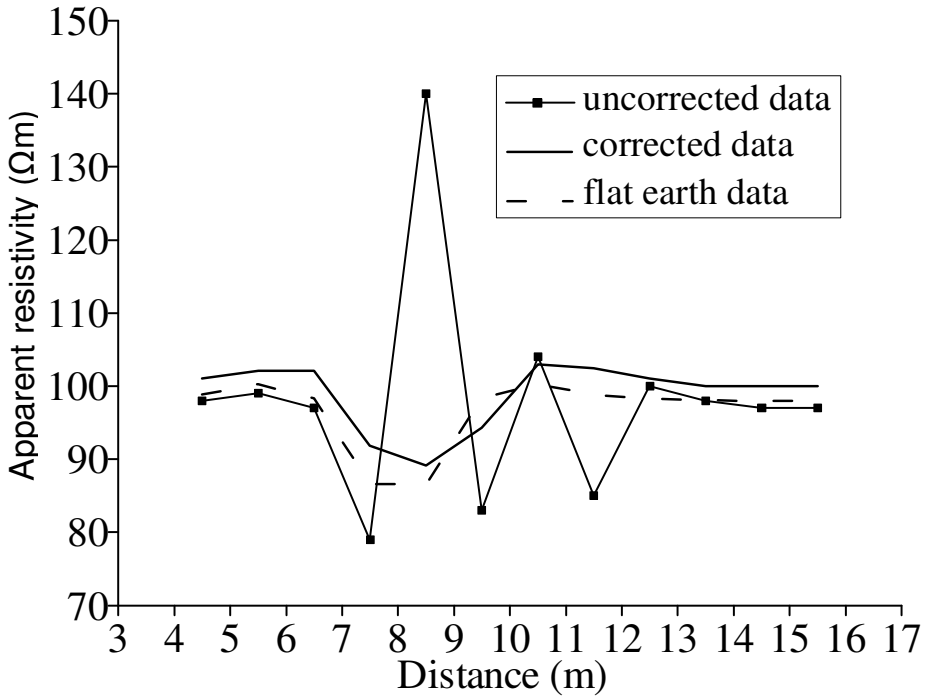

Figure 4. Comparison of the resistivity curves associated with a conductive body for the slope case, uncorrected, corrected and flat earth.

but the amplitudes are increased. This apparent resistivity data is strongly distorted by the slope surface. The major features of the pseudo-section are low near the slope bottom and high near the slope top. To eliminate the slope effect using Equation 3, the ratio of the calculated apparent resistivity pseudo-section (Figure 3c) for the homogeneous topographic model to the model background resistivity (that is 100 Ωm) is multiplied by the observed apparent resistivity pseudo-section (Figure 3b) for the topographic model with the body. The normalized resistivity pseudo-section after the correction is shown in Figure 3d. The slope effect on the pseudo-section was removed along with the normalization and the corrected resistivity pseudo-section shows the response of the buried conductive body. To demonstrate the significance of the normalization procedure, the apparent resistivity curves associated with a buried conductive body for the slope case (Figure 3a), uncorrected (Figure 3b), corrected (Figure 3d) and the response of the same body beneath a flat earth are shown together in Figure 4. The corrected curves compare well with the flat earth curves. The differences remaining are due to the varying distances between the electrodes and the target body.

Inversion incorporating uneven surface

The inversion of the apparent resistivity data is performed incorporating the topography. Figure 5 shows the inversion result for the dipole-dipole array with a slope model. The terrain model (top) under consideration which has a slope of 30° with conductive dike (5 Ωm) in homogeneous ground (100 Ωm) and the observed apparent resistivity pseudo-section (bottom) are shown in Figure 5a. The conductive dike is placed at a depth of 0.5 m under the slope end, having 1 m width and infinite depth extent. The inversion result (top) of the topographic data and the calculated apparent resistivity pseudo-section (bottom) are shown in Figure 5b. Figures 6 and 7 shows the inversion results of the same model in Figure 5, but the homogeneous ground considered as 125 and 150 Ωm, respectively. The previous terrain model is changed to additionally have an overburden with 50 Ωm resistivity and 1 m thickness and the corresponding inversion result is shown in Figure 8. The terrain model (top) and the observed apparent resistivity pseudo-section (bottom) are shown in Figure 8a. The inversion result (top) of the topographic data and the calculated apparent resistivity pseudo-section (bottom) are shown in Figure 8b. The inversion model shows the true locations of the conductive dike and of the overburden, and also agrees with the uniform background, overburden and the target dike resistivities in the terrain model. Figure 9 shows the inversion result of another slope model in which a thin layer with 100 Ωm resistivity and 1 m thickness is added to the latter terrain model. This model represents a geologic model consisting of a decomposed overburden (50 Ωm) over a thin layer (100 Ωm) along

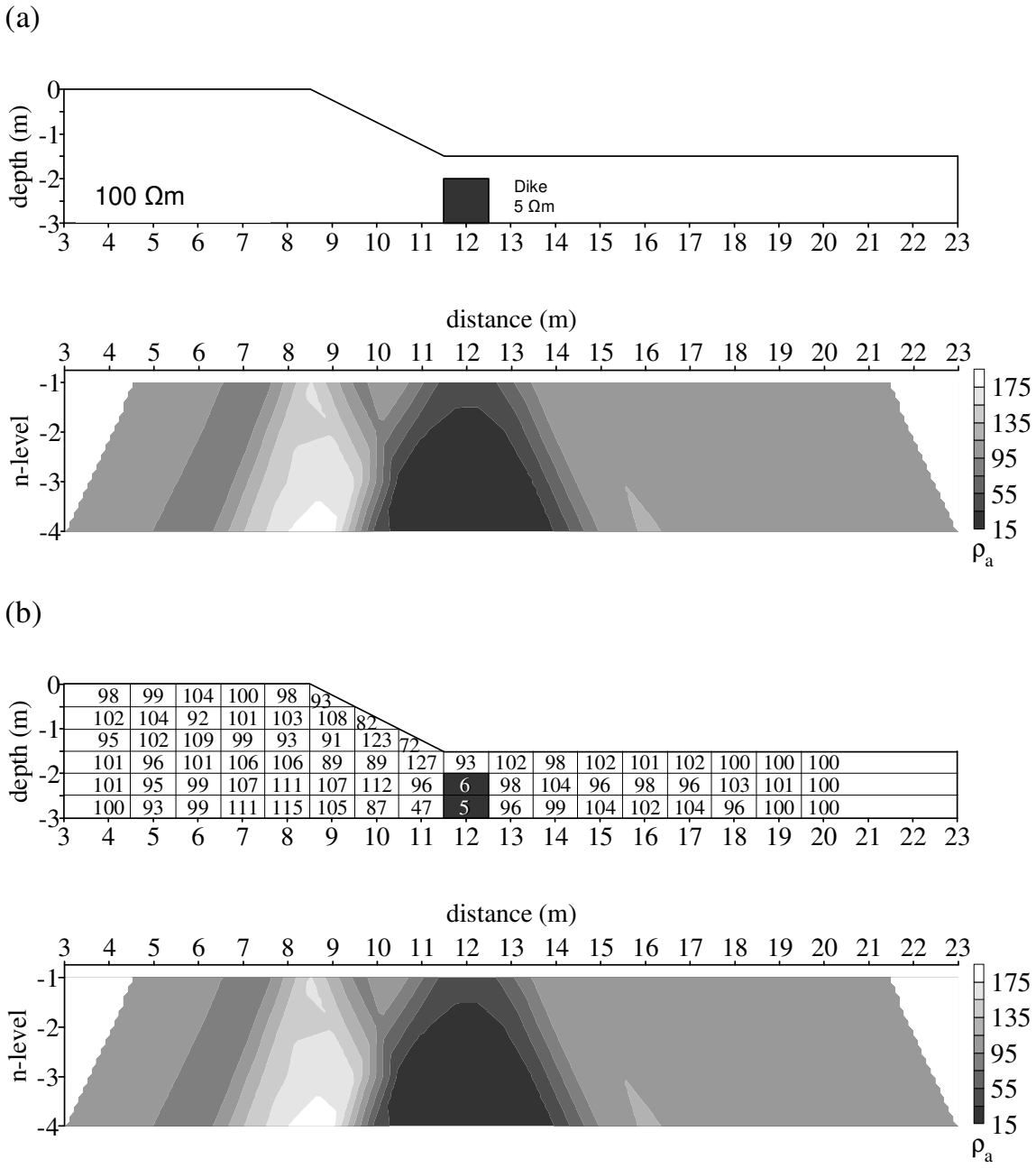

Figure 5. Inversion result of the theoretical apparent resistivity pseudo-section. (a) The slope model (background resistivity is 100 Ωm) with a conductive dike (top) and the observed apparent resistivity pseudo-section (bottom). (b) Inversion model (top) and the calculated apparent resistivity pseudo-section (bottom).

with a conductive dike (5 Ωm) surrounded by a bedrock (300 Ωm). The terrain model (top) and the observed apparent resistivity pseudo-section (bottom) are shown in Figure 9a. The inversion result (top) of the topographic data and the calculated apparent resistivity pseudo-section (bottom) are shown in Figure 9b.

The inversion model agrees with the resistivity distribution in the terrain model. Some artificial high and low resistivity values in the inversion model can be interpreted due to the complexities in the geologic structure not well resolved by the inversion process.

DISCUSSION

The terrain-correction technique and the inversion incorporating topography are the two general approaches used to eliminate the effect of topography on the

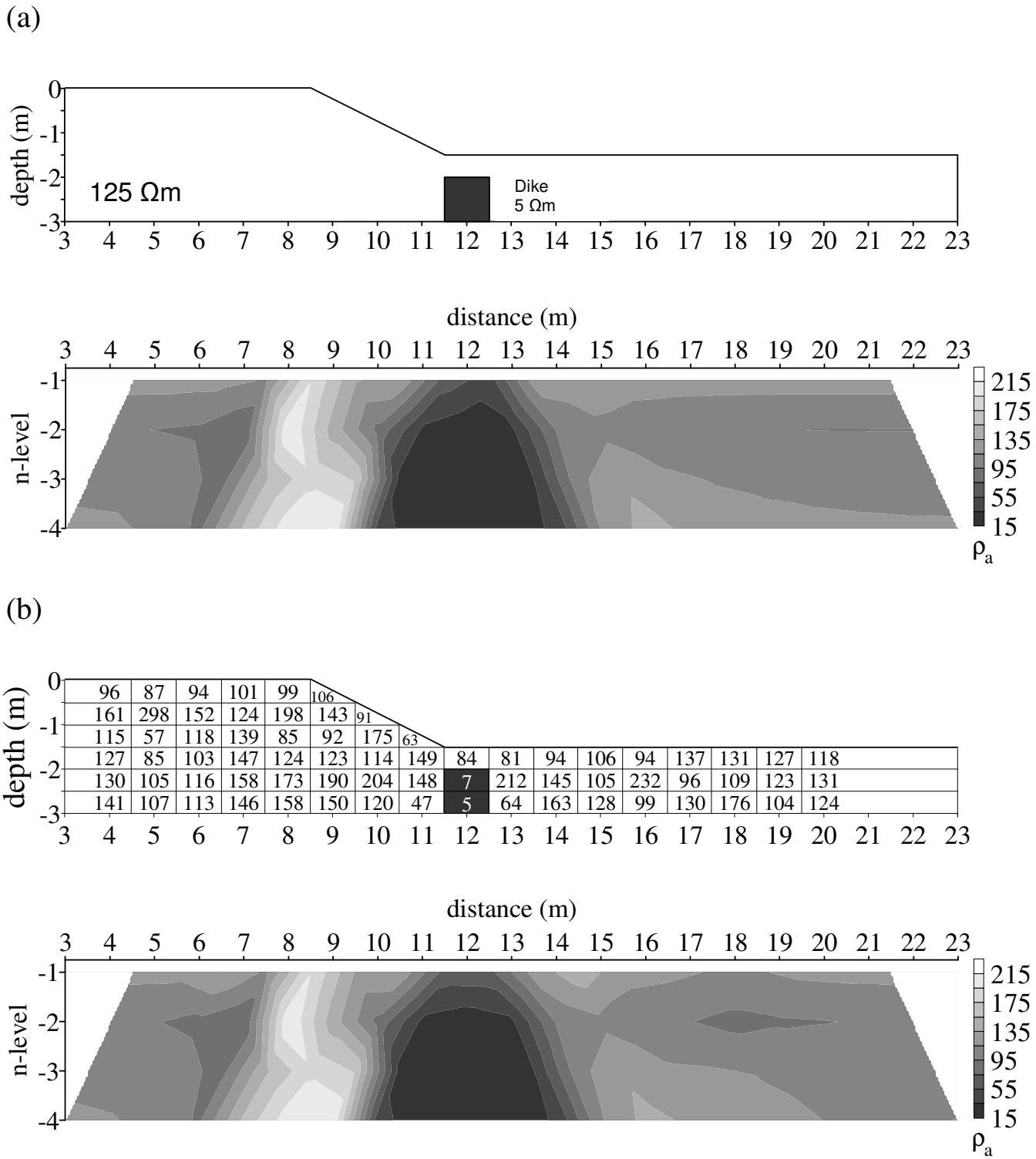

Figure 6. Inversion result of the theoretical apparent resistivity pseudo-section. (a) The slope model (background resistivity is 125 Ωm) with a conductive dike (top) and the observed apparent resistivity pseudo-section (bottom). (b) Inversion model (top) and the calculated apparent resistivity pseudo-section (bottom).

resistivity measurements. We have investigated the effectiveness of these two correction approaches using some theoretical topographic models along with dipole-dipole resistivity responses. The investigations for the hill

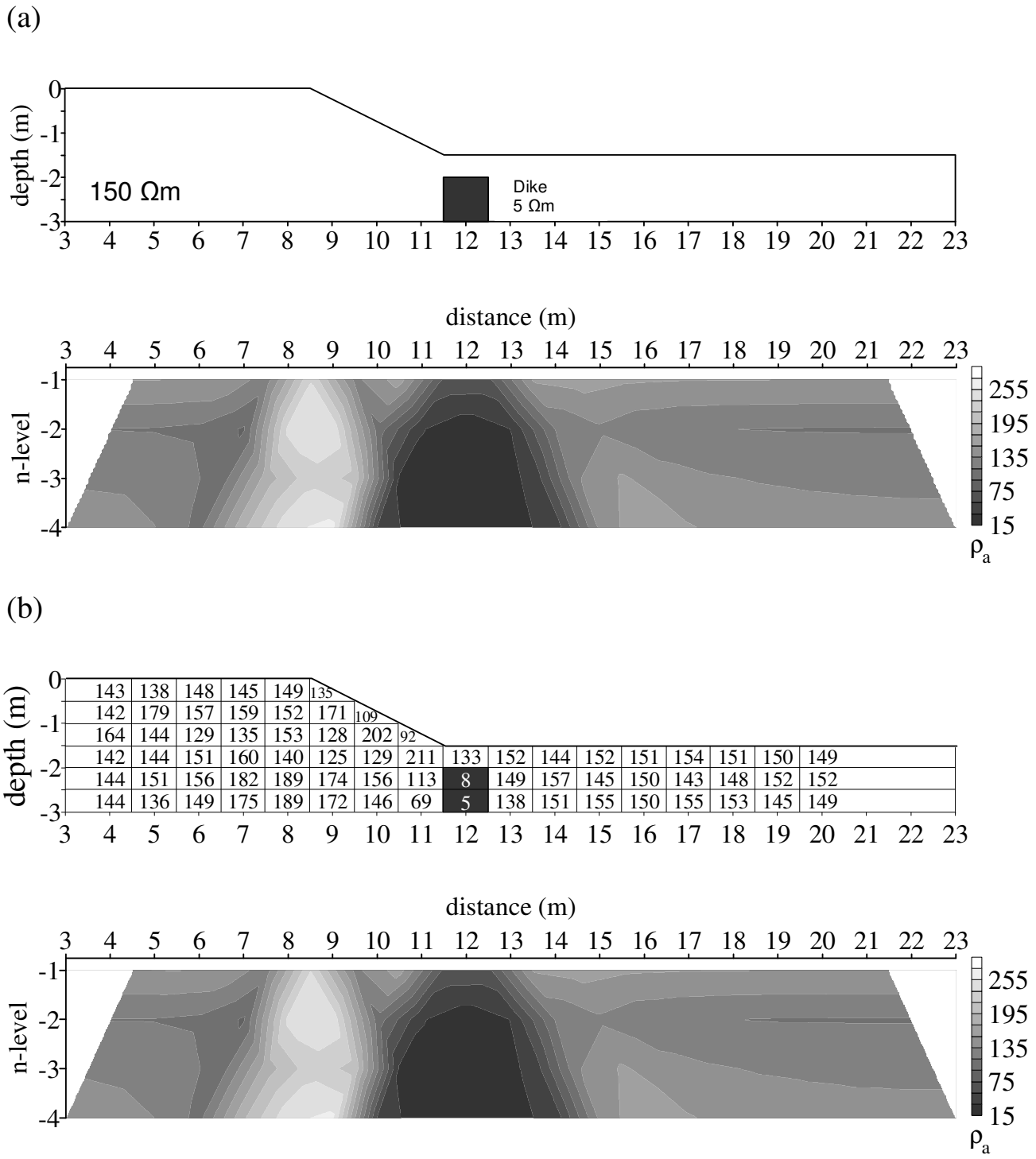

Figure 7. Inversion result of the theoretical apparent resistivity pseudo-section. (a) The slope model (background resistivity is 150 Ωm) with a conductive dike (top) and the observed apparent resistivity pseudo-section (bottom). (b) Inversion model (top) and the calculated apparent resistivity pseudo-section (bottom).

model have shown that the topographic effect becomes larger as the slope angle increases. Topographic correction can be neglected if the terrain surface slopes less than 10°. The corrected apparent resistivity response is much better than the uncorrected resistivity response for a target body under uneven surface. However, when

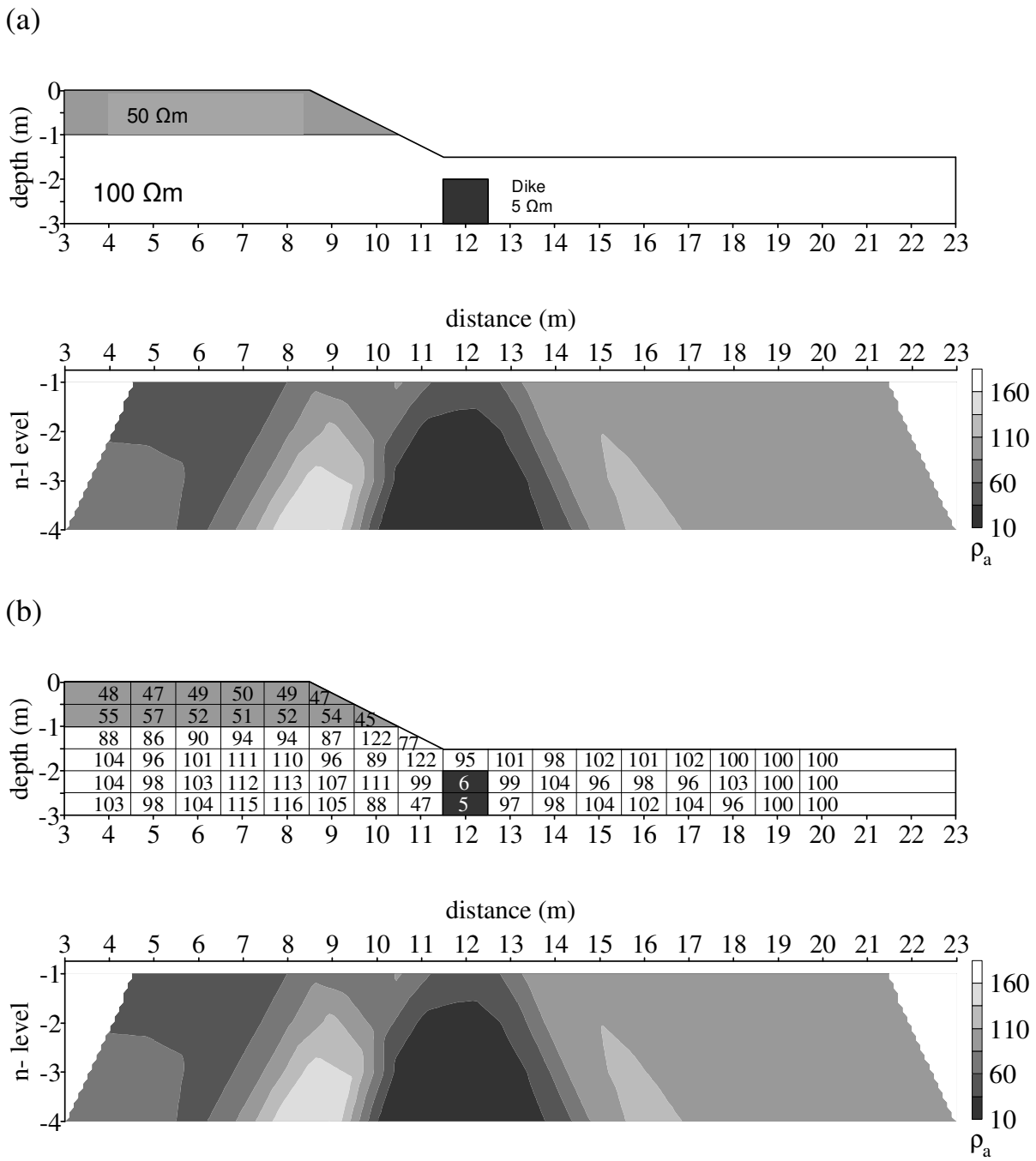

Figure 8. Inversion result of the theoretical apparent resistivity pseudo-section. (a) The slope model including an overburden (top) and the observed apparent resistivity pseudo-section (bottom). (b) Inversion model (top) and the calculated apparent resistivity pseudo-section (bottom).

compared to the flat earth apparent resistivity curves, little differences exist which are due to the varying distances between the electrodes and the target structure. The tests for the slope model have shown that the inversion incorporating topography provides an efficient analysis of the resistivity pseudosections for simple models. The inversion results somehow agree with the modelled resistivity distributions in the terrain models. Some artefacts into the inversion model may exist due to the complexity of the geologic structure. In Figures 5 to 9 the target is conductive dike, contrast with the host rock is very high whose resistivity is 5 Ωm. In inversion models of Figures 5, 6 and 7, the block resistivities are 6.5, 7.5 and 8.5 for host rock of 100, 125

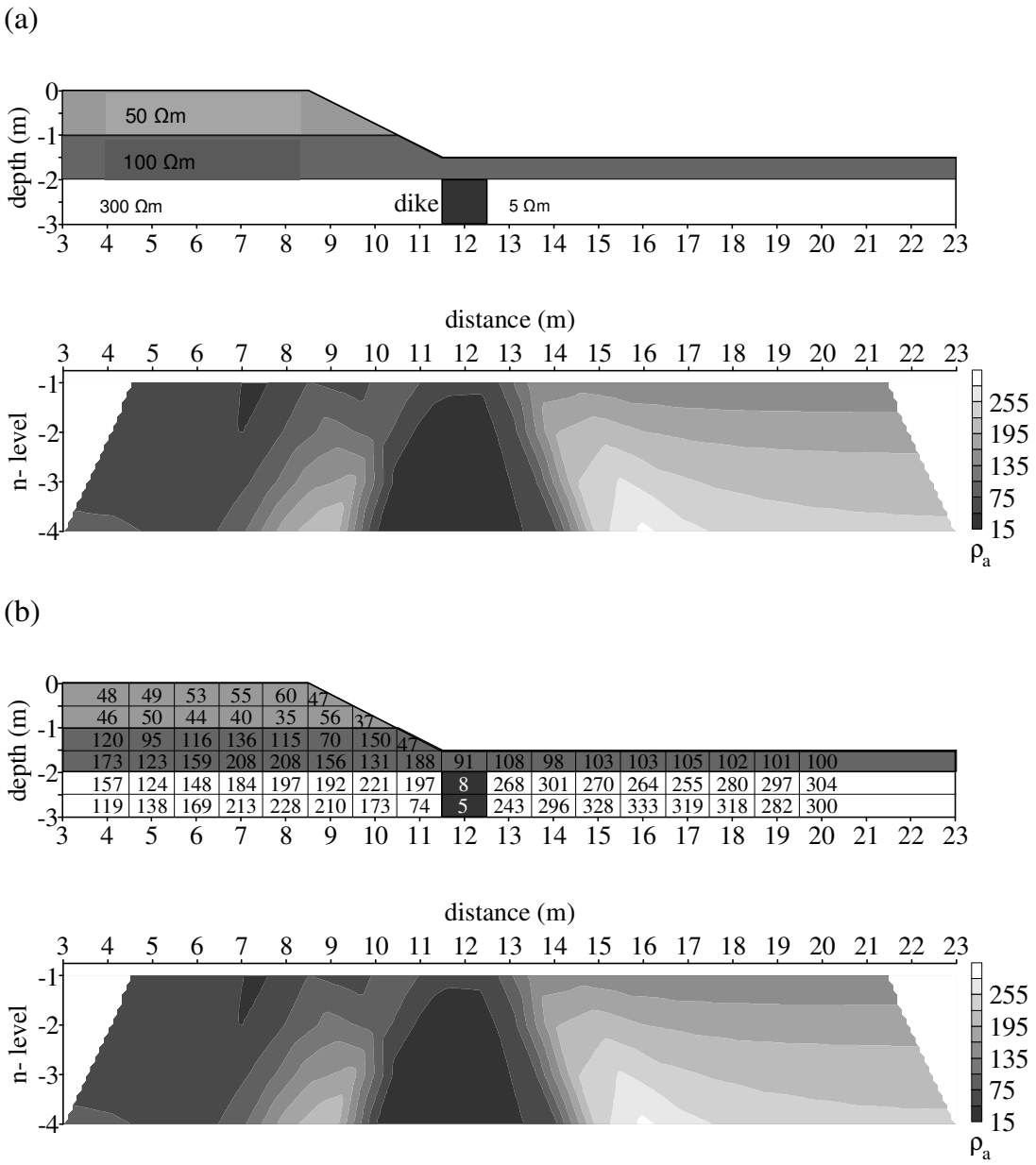

Figure 9. Inversion result of the theoretical apparent resistivity pseudo-section. (a) The slope model (top) and the observed apparent resistivity pseudo-section (bottom). (b) Inversion model (top) and the calculated apparent resistivity pseudo-section (bottom).

and 150 Ωm, respectively. In Figures 8 and 9, inversion results are more erroneous compared with homogeneous background given in Figures 5, 6 and 7.

CONCLUSION AND RECOMMENDATION

The current topographic correction methods are adequate for fairly simple homogeneous host rock having rugged topography. Care should be taken with the application of correction techniques if terrain effects in resistivity responses due to the complex subsurface structures, especially engineering and environmental surveys may not be eliminated completely by the normalization process.

ACKNOWLEDGMENT

The writers thank the anonymous reviewer for the helpful comments that improved the final manuscript.

REFERENCES

Coggon JH (1971). Electromagnetic and electrical modelling by the finite element method. Geophys., 36: 132-155.

Fox RC, Hohmann GW, Killpack TJ, Rijo L (1980). Topographic effects in resistivity and induced polarization surveys. Geophys., 45: 75-93.

Günther T, Rücker C, Spitzer K (2006). Three-dimensional modelling and inversion of dc resistivity data incorporating topography – II. Inversion. Geophy. J. Int., 166(2): 506–517.

Hennig T, Weller A, Canh T (2005). The effect of dike geometry on different resistivity configurations. J. Appl. Geophys., 57: 278-292.

Holcombe HT, Jiracek GR (1984). Three-dimensional terrain corrections in resistivity surveys. Geophys., 49: 439-452.

Loke MH (2000). Topographic modelling in electrical imaging inversion. 62nd EAGE Conf. Tech. Exhib. Glasgow, D2.

Loke MH, Barker RD (1995). Least-squares deconvolution of apparent resistivity pseudosections. Geophys., 60: 1682-1690.

Petrick WR, Pelton WH, Ward SH (1977). Ridge regression inversion applied to crustal resistivity sounding data from South Africa. Geophys., 42: 995-1005.

Queralt P, Pous J, Marcuello A (1991). 2D resistivity modelling: an approach to arrays parallel to the strike direction. Geophys., 56: 941-950.

Rijo L (1977). Modelling of electric and electromagnetic data. Ph.D. Thesis, Univ. Utah, Salt Lake City.

Rücker C, Günther T, Spitzer K (2006). Three-dimensional modelling and inversion of dc resistivity data incorporating topography – I. Modelling. Geoph. J. Int., 166(2): 495–505.

Tong L, Yang C (1990). Incorporation of topography into two-dimensional resistivity inversion. Geophys., 55: 354-361.

Tsourlos P, Szymanski JE, Tsokas G (1998). A smoothness constrained algorithm for the fast 2D inversion of DC resistivity and induced polarization data. J. Balkan Geophys. Soc., 1: 3-13.

Tsourlos P, Szymanski JE, Tsokas G (1999). The effect of topography on commonly used resistivity arrays. Geophys., 64: 1357-1363.

Wannamaker PE (1992). User Documentation: IP2DI-v1.00 finite element program for dipole-dipole resistivity/IP forward modelling and parameterized inversion of two-dimensional earth resistivity structure. Univ. Utah, Salt Lake City.

Xu SZ, Gao Z, Zhao S (1988). An integral formulation for three-dimensional terrain modelling for resistivity surveys. Geophys., 53: 546-552.

Xu SZ, Zhang D, Ruan B, Dai S, Li Y (2002). Calculation of electrical potentials along a longitudinal section of a 2D terrain. Geophys., 67: 511-516.